

Mapping dynamical systems onto complex networks

Ernesto P. Borges^a, Daniel O. Cajueiro^b and Roberto F. S. Andrade^{c*}

^aEscola Politécnica, Universidade Federal da Bahia,
R. Aristides Novis, 2, 40210-630 Salvador–BA, Brazil

^bDepartamento de Economia, Universidade Católica de Brasília
70790-160 Brasília, Brazil

^cInstituto de Física, Universidade Federal da Bahia,
40210-340 Salvador, Brazil

Abstract

A procedure to characterize chaotic dynamical systems with concepts of complex networks is pursued, in which a dynamical system is mapped onto a network. The nodes represent the regions of space visited by the system, while edges represent the transitions between these regions. Parameters used to quantify the properties of complex networks, including those related to higher order neighborhoods, are used in the analysis. The methodology is tested for the logistic map, focusing the onset of chaos and chaotic regimes. It is found that the corresponding networks show distinct features, which are associated to the particular type of dynamics that have generated them.

89.75.Fb: Structures and organization in complex systems

89.75.Hc: Networks and genealogical trees

02.10.Ox: Combinatorics; graph theory

1 Introduction

Chaotic dynamical systems are characterized by several measures that quantify how irregular (despite deterministic) the trajectories are. The set of Lyapunov exponents [1] provides a measure of the dependence on the initial conditions of their trajectories, while information theory may be used to characterize a dynamical system in terms of the production of entropy. Actually, a dynamical system with a chaotic behavior is regarded as a realization of Shannon's concept of an ergodic information source [2], as the Kolmogorov-Sinai entropy

*randrade@ufba.br

is equated [3] to the sum of the positive Lyapunov exponents. Further measures to describe a chaotic system include fractal dimensions and singularity spectra [4, 5]. This formalism applies only where the system has, at least, one positive Lyapunov exponent. However, several authors have studied situations in which the largest Lyapunov exponent vanishes, but the distance between neighbouring trajectories increases in time according to a power law [6, 7, 8, 9]. These situations are usually found at the onset of chaos, where an infinitesimal change of a control parameter drives the system into either a regular or a chaotic regime. These investigations uncovered some of its features related to the sensitivity to the initial conditions [6], entropy production per unit time [10], multifractal geometry of the attractor [11], relaxation to the system attractor [12] and multifractal dynamics at the onset of chaos [13].

Recently, the investigation of complex networks has set up a new framework for the analysis of systems with a large number of degrees of freedom. Within it, one has access to the properties of the topological structure underlying the mutual interactions among the system constituents. This approach has been applied to a large variety of actual systems, ranging from social interactions, biological nature, information and electrical distribution [14, 15].

In this work, we define a mapping of dynamical systems onto a network. This way, the network properties can be used to display new features for the characterization of the system's trajectory. The network nodes correspond to coarse-grained regions (cells) of the phase space visited by the trajectory. Two nodes r and s are linked if, during the time evolution, the trajectory jumps from cell r to cell s . Although this naturally offers a construction procedure for a directed network, we consider here undirected networks. In this approach, we are able to find novel geometric and topological properties of the phase space through the measures that have been recently developed to characterize complex networks. The dynamical system, defined on the time domain, is mapped into a node domain, which represents regions of the phase space visited by the trajectory. As it is based on the division of phase space into boxes, this process follows similar construction procedures considered in the evaluation of the fractal dimension of attractors and the Kolmogorov-Sinai entropy.

It worths mentioning that some previous works have put together ideas of dynamical systems and complex networks. As we shall see, our approach is rather distinct, as the previous contributions consider synchronization under the assumption of certain regularity in the connection topology [16, 17]. The use of a network to represent the phase space evolution of discrete time dynamical systems has been suggested in [18].

We restrict ourselves to the analysis of the quadratic map [19] described by

$$x_{t+1} = 1 - ax_t^2 \quad (t = 0, 1, 2, 3 \dots) \quad (1)$$

where $x_t \in [-1, 1]$ and $a \in [0, 2]$. Eq. (1) leads to a variety of distinct dynamical situations, the properties of which are expected to be manifested in the networks they originate. In particular, we explore those regimes at the onset of chaos that proceed through a bifurcation cascade as well as those close to an intermittency transition and also the full developed chaos.

2 Network characterization

An indirected network R is defined only by the number N of nodes and links L , represented by an assembly of unordered pairs $S_R(r, s)$, $r, s \leq N$, indicating which pairs of nodes are directly connected. This information provides a full description of the network, leading to the computation of the average number of links per node $\langle k \rangle$, the average clustering coefficient C , the mean minimal distance among the nodes $\langle d \rangle$, the diameter D , the probability distribution of nodes with k links $p(k)$. Other measures, like the assortativity degree [20] and the distribution of individual node clustering coefficients $C(k)$ with respect to its degree k have also been introduced, but they are not explored here.

R can be described by its adjacency matrix $M(R)$. This is not the most concise representation of a network, but it opens the possibility to the evaluation of its spectral properties and, as recently indicated, the higher order neighborhoods R_ℓ , $\ell = 1, 2, \dots, D$ [21]. This is done in a straightforward way, by means of the set of matrices $\{M_\ell\}$, so defined that $(M_\ell)_{r,s} = 1$ only if the shortest distance along the network between the nodes r and s is ℓ . Otherwise, $(M_\ell)_{r,s} = 0$. Although the whole information on the network is entailed in $S_R(r, s)$ or in $M(R)$, each M_ℓ condenses information on R that is extracted from $M(R)$ within the quoted framework. This formalism is also consistent with the recently proposed procedure to evaluate the fractal dimension of the network $d_{F,R}$ [22], as it naturally leads to the set $\{N_\ell\}$ required for this evaluation. Here, each N_ℓ counts the number of pairs of nodes which are ℓ steps apart.

Within this framework, we consider that each node is the only zeroth order neighbor of itself, and define $M_0 = I$, where I indicates the identity matrix. Also, we assume that $M_1 = M$. Since the matrix elements of $M(R)$ take only the values 0 and 1, the other matrices M_ℓ of the set are recursively evaluated with the help of Boolean operations [21]. We shall make further use of a matrix that condenses all information in $\{M_\ell(R)\}$. As just discussed, given any two nodes r and s , it is clear that $(M_\ell)_{rs} = 1$ for just one value of ℓ . So, if we define a matrix

$$\widehat{M} = \sum_{j=0}^{\ell_{max}} j M_j, \quad (2)$$

it directly informs how many steps apart any two nodes in the network are. Also, it is possible to use the information in \widehat{M} to graphically display the structure of a network with the help of color or grey scale plots.

It should also be mentioned that this framework opens the door for a finer characterization of the network, if we consider each R_ℓ as an independent network. Thus, several of the properties quoted above used to characterize R can be also evaluated for the evaluation of R_ℓ . This is explored in the next section specifically for the the degree distribution and clustering coefficient $\langle k \rangle_\ell$ and $C(\ell)$.

3 An algorithm to map a dynamical system into a network

To map a dynamical system into a network R , we use the framework of the algorithm introduced in [23], to efficiently evaluate the generalized fractal dimensions of fractal structures by the box counting method.

Let us consider a dynamical system with m variables. Without loss of generality, one can consider a set of points $\mathcal{Z} \subset \mathbb{R}^m$ consisting of the vectors $z(i)$, $i = 1, \dots, T$, $T \gg 1$, which represent the coordinates of the dynamical system. The components of these vectors, $z_\delta(i)$, $\delta = 1, \dots, m$, are assumed to belong to the interval $[0, 1]$. We define a graining in phase space by dividing each phase space axis into W equally sized disjoint intervals, so that the whole phase is spanned by a set of W^m boxes. This represents also the maximal possible number of nodes in a network, as *e.g.*, in the case of an ergodic system. Of course, the choice of W defines the graining, and the size of the region represented by a node. In the next section we investigate the effect of W on the obtained networks.

Based on [23], each point $z(i)$ of the trajectory is mapped into a node of R according to

$$n(i) = \sum_{\delta=1}^m W^{\delta-1} \text{floor}(W z_\delta(i)), \quad (3)$$

where $\text{floor}(x)$ is a function that evaluates the largest integer less than x . Actually, this is just a simple way to divide the region $[0, 1]^m$ in equal parts. Thus, the nodes of the so constructed network represent a box in the coarse grained phase space of the system. After the mapping is complete, the boxes that were not visited by the trajectory are eliminated from the network, as they constitute nodes with zero degree ($k = 0$), which do not provide any useful information on the dynamical system. The edges are built as described in the following procedure. Let $z(i)$ and $z(i+1)$ be two consecutive points of the dynamical system. Suppose that these points were previously mapped into the nodes $n(r)$ and $n(s)$, where $0 < r, s \leq W^m$. Thus, one assumes that there is an edge connecting $n(r)$ and $n(s)$. Here, it is considered that there is only one edge linking $n(r)$ to $n(s)$ if $r \neq s$, *i.e.* self-links are not computed.

This procedure can lead to directed and weighted networks; however, in this work, we focus on the most simple situation of undirected and un-weighted networks, once our main purpose here is to address the problem, and show that we can extract useful information from it.

4 Results

We concentrate our investigation on three distinct regions of a , $a = a_c = 1.40115518909\dots$, $a \in [1.749, 1.75)$ and $a = 2$, which correspond, respectively, to the first period doubling transition, the region close to the tangent bifurcation

to the period-three window, and the full developed chaotic state. Representative networks to the distinct chaotic attractors are generated for distinct values of the graining W . We only consider trajectories that start on the attractor, in order to avoid spurious nodes (visited only once) that depend on initial conditions. For a fixed value W , the network grows as the trajectory evolves in the phase space with respect to the number of iteration steps t . There is no a priori criterion to decide the time t_F after which the network is complete. In this work we have followed how N and L increase with t , for a given W . We define t_F as the smallest value of t for which $N(t_F) = N(2t_F)$ and $L(t_F) = L(2t_F)$.

First let us discuss the effect of W on N and L . For the purpose of presenting a full neighborhood analysis of the networks, we have selected here values of W that lead to the maximal number ≈ 10000 nodes in the network. Such choice for W clearly depends on a . Indeed, due to the strategy adopted for the construction of the networks, N grows with W according to a power law mediated by the fractal dimension of the attractor $d_{F,A}$. This is shown in Fig. 1a, where we draw points for $a = a_c$, $a_c + 10^{-3}$, 1.749999 and 2. For a_c we measure the slope 0.54..., which agrees with the known value of $d_{F,A}$ of the period doubling attractor. For all other cases, the slope is 1 within 2% accuracy, even for $a = a_c + 10^{-3}$, which lies already in the chaotic regime. This is in accordance with the fact that $d_{F,A}$ changes in a discontinuous way at $a = a_c$. When a corresponds to a periodic solution, the network becomes finite, so that N and L do not depend on W , provided this parameter is large enough.

Although we are primarily interested in the properties of the complete network, we can also follow the dependency of N and L with respect to t , for a fixed value of W . Assuming $N \sim L^z$, this defines a dynamical exponent z in the early stages of the network evolution. The analyzed data indicate that $z \simeq 1$ for all values of a . Nevertheless, we find that, in the immediate chaotic neighborhood of $a = 1.75$, the laminar phases in the intermittent regime traps the trajectory for long intervals, demanding large time of integration to complete the network.

Now we discuss the network properties, following the methodology and parameters indicated before. When appropriate, we extend our discussion to properties of higher order neighborhoods in the network. We find distinct network structures when we consider the chaotic regime or the onset of chaos. Regarding the mean minimal distance $\langle d \rangle$ and diameter D , we find that, for the chaotic regime, they grow with respect to W (and N), in a logarithmic way, similarly to small-world networks [24]. If we write $\langle d \rangle = \alpha \log_{10} W$, we find $\alpha \simeq 2.4$ and 3.7, respectively, for $a = 2$ and $a \in [1.749, 1.749999]$, as illustrated in the inset of Fig. 1b. As D only assumes integer values, it is possible to expect a similar behavior only in an approximate way, *e.g.*, equally sized steps in $D \times \log_{10} W$ plots. Thus, assuming $D = \beta \log_{10} W$, we find $\beta \simeq 4$ for $a = 2$ with very good accuracy. In the interval $[1.749, 1.749999]$, we noticed the presence of fluctuations in the size of the steps, which increases when we approach the threshold $a = 1.75$. The results for $a = a_c$ have a completely distinct behavior: $\langle d \rangle$ and D increase as power laws with respect to W , as illustrated in the main panel of Fig. 1b. For $a = a_c + 10^{-3}$, the same dependence prevails. The exponents

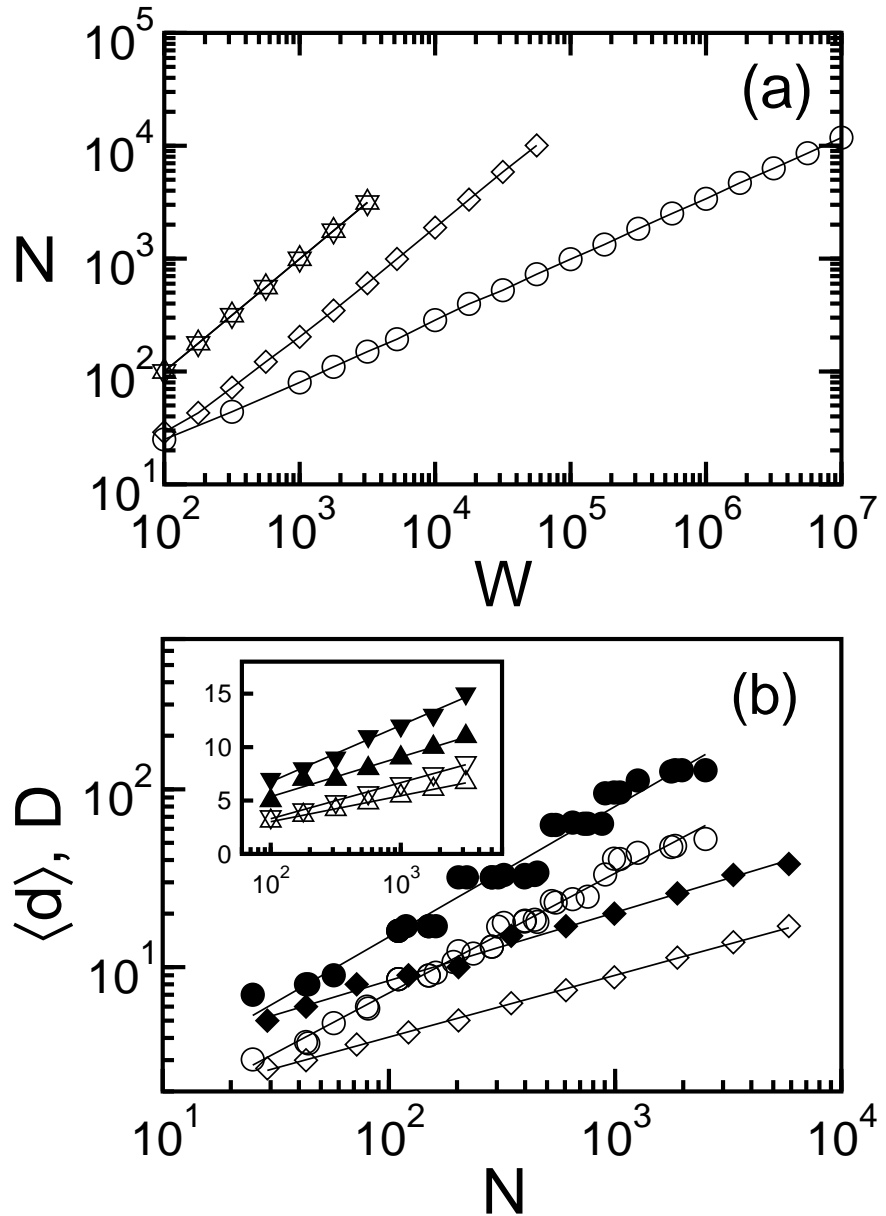


Figure 1: (a) Dependence of N with respect to W for $a = a_c$ (circles), $a = a_c + 10^{-3}$ (diamonds), $a = 1.749999$ (down triangles), and $a = 2$ (up triangles). The same convention is used in all other figures. The distinct slopes indicate the values of $d_{F,A}$. (b) Power law dependence of $\langle d \rangle$ (hollow symbols) and D (solid symbols) with respect to N for $a = a_c$ and $a = a_c + 10^{-3}$. The inset shows logarithmic dependence among the same quantities when $a = 1.749999$ and $a = 2$.

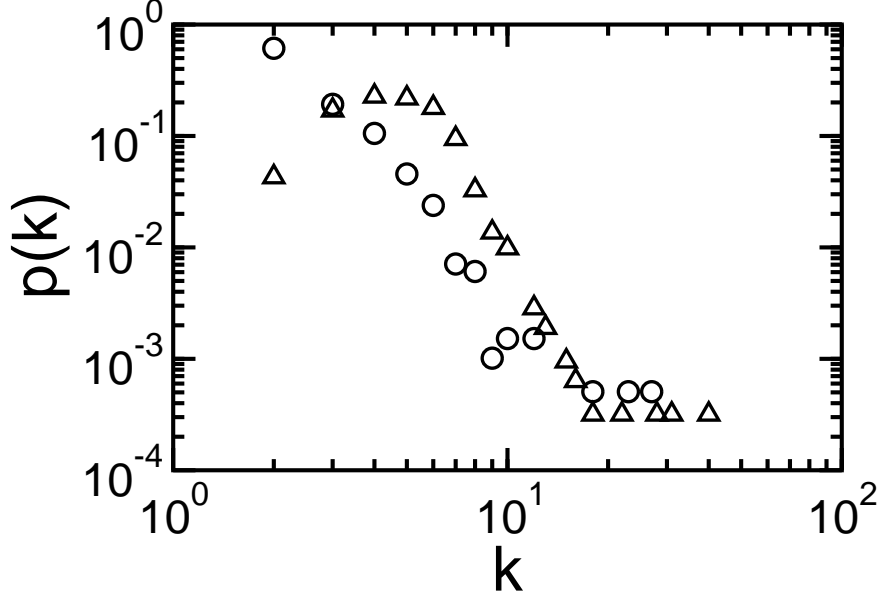


Figure 2: Degree distribution of nodes at a_c (circles) and in the $a = 2$ chaotic regime, (up triangles). Behavior close to tangent bifurcation, $a = 1.75 - 10^{-4}$, (not shown) is quite similar to $a = 2$.

obtained for $\langle d \rangle$ and D are, respectively, 0.67 and 0.73 for a_c , and 0.35 and 0.38 for $a = a_c + 10^{-3}$. $\langle d \rangle$ and D increase smoothly for $a = a_c + 10^{-3}$ but at $a = a_c$, the growth of the two quantities present discontinuities and steps. Results in Fig. 1b indicate that, unlike the properties of the attractor, reflected by the rash change in the value of $d_{F,A}$, the network properties change slowly when the chaotic regime is reached.

We have evaluated the distribution $p(k)$ vs. k in all different regimes. We can see in Fig. 2 that, for $a = a_c$, k does not reach large values ($k_{max} \simeq 30$), so that it is not possible to identify a power law decay in this range. For $a = 2$ (and also $a = 1.749999$) nodes with larger values of k can be found, but $p(k)$ does not follow either a power law.

Such distinct behavior is also explicit when we analyze the fractal dimension of the network $d_{F,R}$ [22]. Fig. 3 shows that the $a = a_c$ networks have a well defined scaling behavior, which extends over more than two decades, in a quite precise way. On the other hand, a fractal dimension for the networks in the chaotic regime is not evident. First, the small values of D reduces the region of possible scaling behavior. Then, we clearly observe deviations to the expected power-law regime.

Regarding the clustering coefficient, we obtain $C \equiv 0$ for $a = a_c$, indicating the complete absence of triangles in the network. For $a = 1.749999$ and $a = 2$,

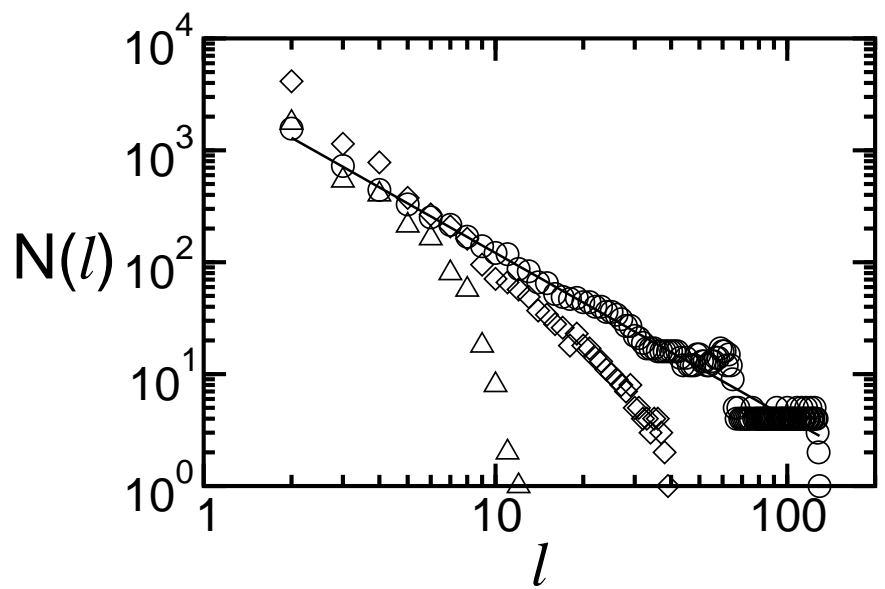


Figure 3: Clear power law behavior for $N(\ell) \times \ell$ when $a = a_c$, with $d_{F,R} = 1.47$. Finite size effects blur this dependence when $\ell \simeq D$. In the chaotic regime, for $a = 2$, $d_{F,R}$ can hardly be evaluated. For $a = a_c + 10^{-3}$, the points illustrate a slow transition between the two regimes.

we find that C decays with N according to a power law with exponent ≈ 0.95 , what is not so close to the value 0.75 observed for the Albert-Barabasi scale-free network [14]. However, its small values indicate that the network has only a small number of triangles.

Other features of the network may be drawn if we consider the clustering coefficient of higher order neighborhoods [21]. To obtain a clearer picture of this analysis consider, for instance, the regular Cayley tree with $\ell = 2$ network for the complete regular three neighbors Cayley tree. The $\ell = 2$ network is formed by triangles, much like the Husimi cactuses and, correspondingly, a large value for $C(\ell = 2)$. The following odd and even numbered neighborhoods are characterized, respectively, by values of $C(\ell) = 0$ and $C(\ell) > 0$, whereby the values of $C(\ell)$ for a subset of even neighborhoods decrease in a monotonic way. A similar situation is found for the networks investigated here. In Fig. 4a we summarize the sequence of $C(\ell)$ for the three situations under investigation. We see that, for $a = 2$ and $a = 1.4999$, the oscillatory behavior lasts only until $\ell = 5$ and 10, respectively. Also we note that the odd numbered $C(\ell)$ increases until it reaches values as high as those of the even numbered neighborhoods. On the other hand, the $a = a_c$ network has $C(\ell) = 0$ for all odd numbered neighborhood. The inset shows that the $C(\ell = \text{even number})$ decays with ℓ according to a power law, with exponent $\alpha \simeq 1$.

We have also analyzed the average degree $\langle k \rangle_\ell$ as a function of the neighborhood ℓ . Here again we find that the behavior of the chaotic regime and the onset of chaos have distinct features, as exhibited in the Fig. 4b.

Finally, we use the information in \widehat{M} to obtain images, in color (or gray) scale, of the network neighborhood structure. They provide a vivid and easy visualization of their distinct properties of the attractor. For $a = 2$, the first order neighborhood is distributed along the parabola described by the r.h.s. of (1) (see Fig. 5a). It shows how the second and higher order neighborhood evolve according to the higher order iterates of the quadratic map. However, mixing and finite size effects stemming from a finite graining smears the higher order iterates. The situation is distinct for a_c , when the attractor is a $d_{F,A} = 0.54\dots$ dust spread out in the $[-1, 1]$ interval. Only boxes containing part of the dust remain in the network, so that contiguous numbered nodes are not actually neighbors in phase space. The resulting image (Fig. 5b) displays a fine and intertwined tessitura that reflects a very peculiar behavior of the trajectories at the onset of chaos[7, 8, 9].

5 Conclusion

In this work we explore the idea of mapping chaotic systems onto complex networks. Networks are constructed according to a well defined methodology, and results for the logistic map indicate how their properties can be associated to those of the attractor in phase space. Trajectories in distinct dynamical regimes are explored in order to show how the major differences in phase space are reflected in the networks. The networks show several features of small-world and

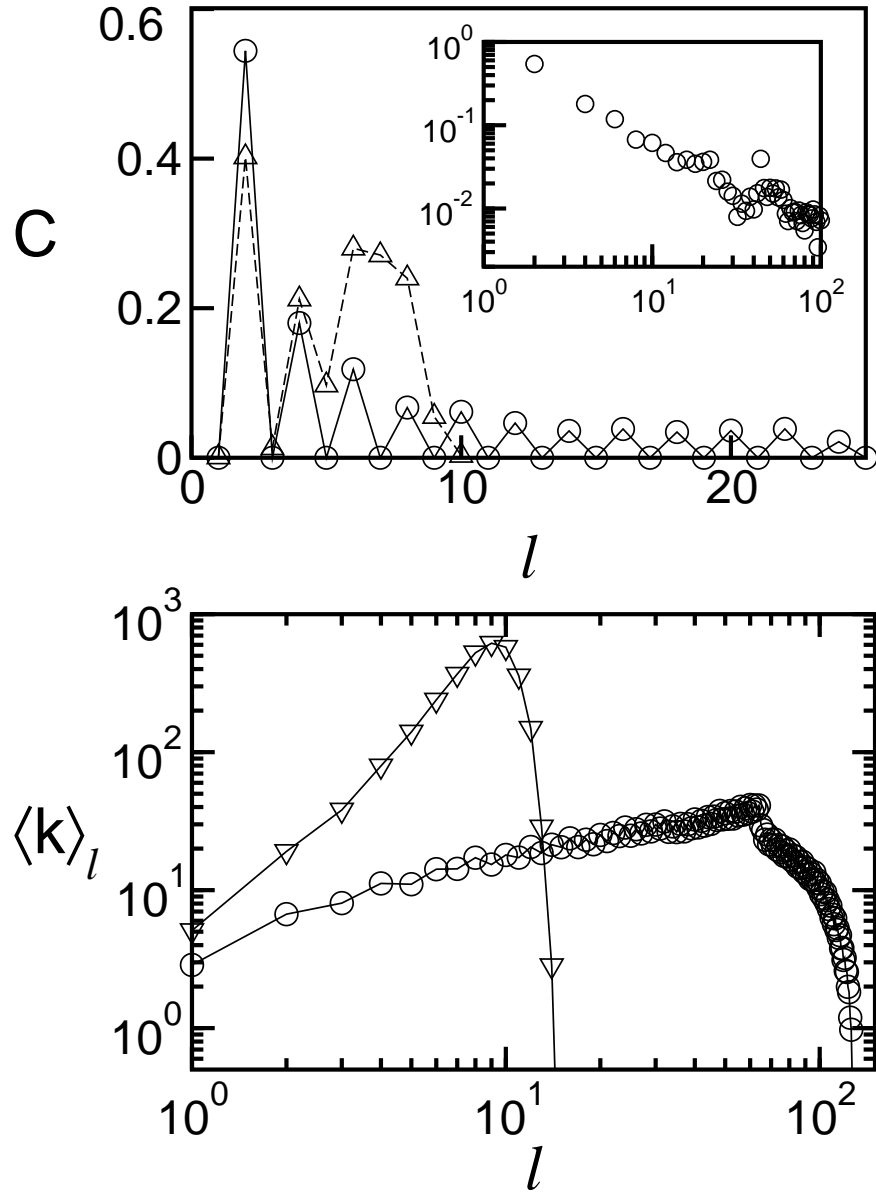


Figure 4: (a) Behavior of $C(\ell)$ with respect to ℓ for chaotic regime and at the onset of chaos. The inset shows a peculiar power law behavior $C(\ell)$ at the onset of chaos. (b) Behavior of $\langle k \rangle_\ell \times \ell$. The onset of chaos exhibits a slow increasing value of $\langle k \rangle_\ell$ over a large interval of ℓ , interrupted by finite size effects already present in Fig. 3. In opposition to this picture, chaotic regime shows a sharp increase of $\langle k \rangle_\ell$.

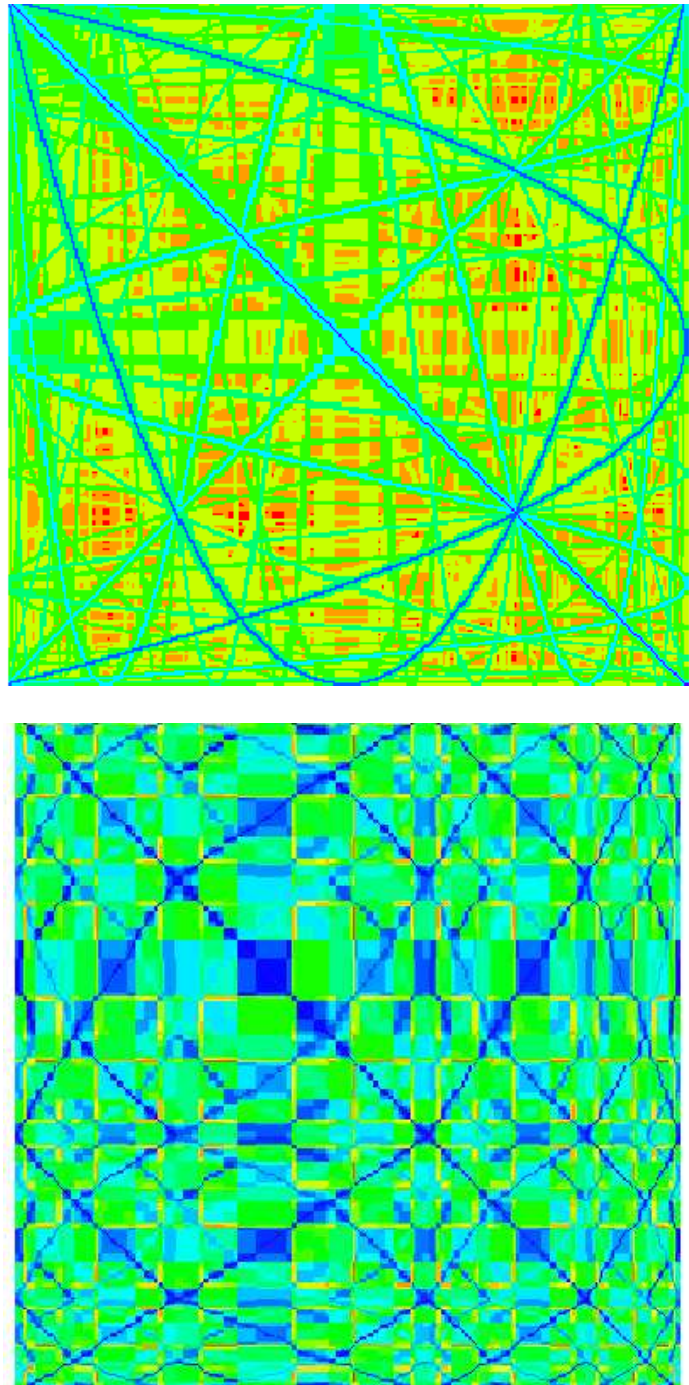


Figure 5: Color scale plots (gray scale in paper version) of \widehat{M} for $a = 2$ (a) and $a = a_c$ (b). Scale ranges from black and blue ($\ell = 0$ and $\ell = 1$) to red ($\ell = D$). Number of levels in (a) is much smaller than in (b). Neighborhood structure changes abruptly in the distinct regimes.

scale-free networks, but they do not fully match with those networks generated by the specific algorithms described in [24, 25]. The analysis of the networks in the neighborhood of a_c reveals that the $N \times W$ dependence, measured by $d_{F,A}$, has a sharp transition at the onset of chaos. So, the distinct character of the trajectories in phase space is indeed reflected in the network. However, with exception of C , the results for the other indices ($\langle d \rangle$, D and $p(k)$) change in a much smoother way with respect to changes in the parameter a .

Acknowledgements: This work was supported by the Brazilian Agencies CNPq and FAPESB.

References

- [1] Eckmann J. P. Ruelle D., Rev. Mod. Phys. **57**, (1985) 617.
- [2] Gallager R. G., *Information theory and reliable communication* (Addison-Wesley, Reading, MA 1968).
- [3] Pesin Y. B., Rus. Math. Surv. **32**, (1977) 55.
- [4] Hentschel H. G. E. Procaccia I., Physica D **8**, (1983) 435.
- [5] Meneveau C. Sreenivasan K. R., Phys. Lett. A **137**, (1989) 103.
- [6] Tsallis C., Plastino A. R. Zheng W. M., Chaos Solitons and Fractals **8**, (1997) 885.
- [7] Baldovin F. Robledo A., Phys. Rev. E **69**, (2004) 045202.
- [8] Robledo A., Europhys. News **36**, (2005) 214.
- [9] Hernández-Sandaña H., Robledo A., Physica A **370**, (2006) 286.
- [10] Latora V., Baranger M., Rapisarda A. Tsallis C., Phys. Lett. A **273**, (2000) 97.
- [11] Lyra M. L. Tsallis C., Phys. Rev. Lett. **80**, (1998) 53.
- [12] Borges E. P., Tsallis C., Ananos G. F. J. de Oliveira P. M. C., Phys. Rev. Lett. **89**, (2002) 254103.
- [13] Mayoral E. Robledo A., Phys. Rev. E **72**, (2005) 026209.
- [14] Albert R. Barabasi A.-L. , Rev. Mod. Phys. **74**, (2002) 47.
- [15] Boccaletti S., Latora V., Moreno Y., Chavez M. Hwang D. U., Phys. Rep. **424**, (2006) 175.
- [16] Pikovsky A., Rosenblum M. Kurths J., *Synchronization - a universal concept in nonlinear science* (Cambridge University Press, Cambridge 2001).
- [17] Atay F. M. Jost J., Phys. Rev. Lett. **92**, (2004) 144101.

- [18] Thurner S., *Europhys. News* **36**, (2005) 218.
- [19] Collet P. Eckman J. P., *Iterated Maps on the Interval as Dynamical Systems* (Birkhauser, Boston 1980).
- [20] Newman M. E. J., *Phys. Rev. Lett.* **89**, (2002) 208701.
- [21] Andrade R. F. S., Miranda J. G. V. Lobão T. P., *Phys. Rev. E* **73**, (2006) 046101.
- [22] Song C. M., Havlin S. Makse H. A., *Nature* **433**, (2005) 392.
- [23] Block A., Von Bloh W. Schellnhuber H. J., *Phys. Rev. A* **42**, (1990) 1869.
- [24] Watts D. J. Strogatz S. H., *Nature* **393**, (1998) 440.
- [25] Barabasi A.-L. Albert R., *Science* **286**, (1999) 509.